Article

Enhanced Expression of CD13 in Vessels of Inflammatory and Neoplastic Tissues

Paola Di Matteo, Gian Luigi Arrigoni, Luca Alberici, Angelo Corti, Corrado Gallo-Stampino, Catia Traversari, Claudio Doglioni[1], and Gian-Paolo Rizzardi[1]

MolMed SpA, Milan, Italy (PDM,CGS,LA,CT,GPR), Vita-Salute University (PDM), Division of Molecular Oncology (AC), and Department of Pathology (GLA,CD), San Raffaele Scientific Institute, Milan, Italy.

Summary

Aminopeptidase-N (CD13) is an important target of tumor vasculature-targeting drugs. The authors investigated its expression by immunohistochemistry with three anti-CD13 monoclonal antibodies (WM15, 3D8, and BF10) in normal and pathological human tissues, including 58 normal, 32 inflammatory, and 149 tumor tissue specimens. The three antibodies stained vessels in most neoplastic tissues, interestingly with different patterns. As a matter of fact, WM15 stained almost all intratumor and peritumor capillaries and only partially large vessels, whereas BF10 and 3D8 reacted with arteries and venules and to a lesser extent with capillaries. These antibodies also stained the stroma in about half of neoplastic tissues. In inflammatory lesions, the three antibodies stained vessels and stroma, whereas in normal tissues, they stained a small percentage of blood vessels. Finally, the three antibodies failed to stain endothelial cells of normal colon, whereas they reacted with activated human umbilical vein endothelial cells and with endothelial cells of colon adenocarcinoma vessels. Overall, WM15 was the most specific antibody for angiogenic tumor vessels, suggesting that it may be a good tool for detecting the CD13 form associated with the tumor vasculature. This finding may be relevant for CD13-mediated vascular targeting therapies. (J Histochem Cytochem 59:47–59, 2011)

CD13/aminopeptidase N is a heavily glycosylated, ~150–240-kDa, type-II membrane, expressed by most cells of myeloid origin including monocytes, macrophages, granulocytes, and their hematopoietic precursors (Chen et al. 1996; Riemann et al. 1999; Mina Osorio 2008). It is also abundantly expressed in the brush border of epithelial cells from renal proximal tubules and small intestine, in prostatic epithelial cells, in bile duct canaliculi, in mast cells, and, in some cases, in fibroblasts and smooth muscle cells (Taylor 1993; Dixon et al. 1994; Riemann et al. 1999; Mina Osorio 2008). Of note, CD13 is a multifunctional protein and plays varying roles in cell migration, cell proliferation, cell differentiation, antigen presentation, protein degradation, cytokine and neuropeptide regulation, extracellular matrix degradation, and tumor invasion and as a viral receptor (Razak and Newland 1992a, 1992b; Riemann et al. 1999; Luan and Wu 2007; Mina Osorio 2008; Wulfaenger et al.

2008). Importantly, CD13 participates in angiogenesis generating and modulating angiogenic signals, in the process of capillary tube formation, and as a marker of angiogenic vessels (Pasqualini et al. 2000; Bhagwat et al. 2001, 2003; Bauvois 2004; Bauvois and Dauzonne 2006; Fukasawa et al. 2006; Mahoney et al. 2007; Yang et al. 2007; Mina Osorio 2008). In addition, inhibition of CD13 with either anti-CD13 antibodies or with bestatin impairs angiogenesis, whereas hypoxia and

angiogenic factors induce CD13 expression in endothelial cells (Bhagwat et al. 2001; Mina Osorio 2008); finally, CD13-null mice show reduced angiogenic responses to growth factors and are significantly deficient in promoting retinal neovascularization under hypoxic conditions (Rangel et al. 2007). Overall, these data indicate that CD13 exerts key roles in angiogenesis.

It has recently been demonstrated that phages expressing the amino acid sequence Asp-Gly-Arg (NGR) can bind CD13 (Pasqualini and Ruoslahti 1996; Pasqualini et al. 2000; Arap et al. 2002). Different CD13 forms are expressed within tumor vessels, normal epithelia, and myeloid cells (Curnis, et al. 2002), providing support for varying ligand specificities. Furthermore, the NGR motif can bind to vessels within or close to tumor nodules but not to vessels or epithelia in normal tissues (Curnis, Arrigoni, et al. 2002). On the basis of these observations, it has been suggested that the tumor-homing properties of the NGR peptides rely on recognition of a CD13 form selectively expressed within tumor-associated vessels (Curnis, et al. 2002).

In this study, we investigated the expression of CD13 in several human tumor, inflammatory, and normal tissues using three different monoclonal antibodies (mAbs; WM15, BF10, 3D8). We show that the expression of CD13 is enhanced in the vasculature of most neoplastic tissues, of some inflammatory lesions, whereas it is almost undetectable in the vasculature of most normal tissues.

Material and Methods

Tissues

Unfixed surgical specimens from different organs and skin biopsies were rapidly sent to our pathology department. Upon gross examination, either nonneoplastic or neoplastic areas from the same specimen were separately collected, snap frozen, and stored at −70C. Frozen sections (3–5 μm) were air dried for 30 min and fixed with paraformaldehyde for 20 min at 4C. Specimens analyzed included 239 human specimens (frozen sections), represented by 58 normal, 32 inflammatory, and 149 tumor tissues (Tables 1–3). For each case, diagnosis was established on routine paraffin-embedded material according to standard histopathologic criteria. Protocols for taking the specimens from patients have been performed in accordance with the Helsinki Declaration of 1975 and the San Raffaele Hospital Review Board.

Immunohistochemistry Procedure

Immunohistochemical analysis was performed with the following three anti-CD13 mAbs: WM15 (1:5000, mouse $IgG_1\kappa$; BD Pharmingen, Franklin Lakes, NJ), 3D8 (1:100, mouse $IgG_1\kappa$; Thermo Scientific, Waltham, MA), and BF10 (1:100, mouse $IgG_1\kappa$; Thermo Scientific). WM15 recognizes an epitope in the vicinity of the catalytic site, whereas 3D8

recognizes a different epitope lying outside the catalytic site (Ashmun et al. 1992); the BF10 epitope is unknown. Unlike WM15, BF10 and 3D8 can be used in Western blot analysis. The epitope recognized by WM15 is destroyed during the process of formalin fixation and paraffin embedding. Therefore, we performed all immunostainings with the three mAbs using frozen sections. Finally, the three mAbs have been raised against different tumor cells (mAb data sheets). Detection was performed with Super Sensitive Polymer-HRP IHC Detection Systems (Biogenex, San Ramon, CA), according to the manufacturer's instructions, followed by chromogenic reaction with diaminobenzidine (DAB chromogen, cod. K3468; DakoCytomation, Fort Collins, CO); the slides were counterstained with Harris hematoxylin for 10″. Negative controls were performed by omitting the primary antibody. The immunostaining of each tissue was evaluated independently by two of us (G.L.A. and P.D.M.), and consensus was reached for discordant cases. We semiquantitatively defined the grading as follows: >80% (+++), 40–80% (++), 10–40% (+), <10% (+/−) positive cells; no staining (−). In the summary tables (Tables 1–3), the immunostaining "+", "++," and "+++" were considered positive, whereas the staining "+/−" and "−" were considered negative.

Immunofluorescence Staining

To demonstrate co-localization between CD13 and vessels, selected samples were stained with anti-CD13 and anti-CD31 by immunofluorescence. Frozen sections were blocked with 1% bovine serum albumin and 5% fetal bovine serum (FBS). Sections were then stained with the following antibodies: anti-CD13, WM15-Alexa Fluor 488 (mouse IgG_1; Axxora, Lausen, Switzerland), and anti-CD31 (rabbit polyclonal; Thermo Scientific) antibody followed by anti-rabbit AlexaFluor 555-conjugated antibodies (Invitrogen, Carlsbad, CA). The results were observed, and the images were captured with a Nikon 80iEclipse fluorescent microscope.

Flow Cytometry

Flow cytometry analysis (FACSCalibur; BD Biosciences, Franklin Lakes, NJ) was performed on $CD31^+CD45^-$ endothelial cells identified with mouse anti-human FITC-CD31 ($IgG_1\kappa$, clone WM59; BD Biosciences) and mouse anti-human PerCP-CD45 ($IgG_1\kappa$, clone 2D1; BD Biosciences) mAbs in homogenized human tissue specimens of paired normal colon and colon adenocarcinoma ($n = 2$) and on endothelial cells isolated from the vein of the umbilical cord (human umbilical vein endothelial cells [HUVEC]; PromoCell, Heidelberg, Germany).

Immediately after sampling, fresh normal colon and colon adenocarcinoma tissue specimens were homogenized with a 1-mg/ml mix of A and B collagenases (Roche, Basel, Switzerland) for 90 min at 37C, followed by mechanic cellularization and 40μ filtration. Cells ($5–10 \times 10^5$) were then

Table 1. Immunohistochemical Analysis of CD13 Expression in 149 Tumor Tissue Specimens

		Monoclonal Antibody														
		WM15					BF10					3D8				
Tissues	n	Vessels	Tumor Cells	Stroma	Adjacent Normal Tissues	n	Vessels	Tumor Cells	Stroma	Adjacent Normal Tissues	n	Vessels	Tumor Cells	Stroma	Adjacent Normal Tissues	
Liver																
Hepatocarcinoma	2	+	+	+	–	0					0					
Nodular hyperplasia	1	+	+	–	+	0					0					
Metastases of colon adenocrcinoma	7	++	–	+	+	0					0					
Metastases of melanoma	1	+	+	–	–	0					0					
Total	11	11/11	4/11	9/11	8/11	0					0					
Bowel																
Colon adenocarcinoma	11	++	–	+	+/-	3	+++	–	+	+/-	3	+++	–	+	+/-	
Sigma adenocarcinoma	1	–	–	+	+/-	0					0					
Rectum adenocarcinoma	1	+	–	–	+/-	0					0					
Total	13	12/13	0/13	12/13	0/13	3	3/3	0/3	3/3	0/3	3	3/3	0/3	3/3	0/3	
Breast																
Ductal carcinoma	8	++	–	+	–	0					0					
Lobular carcinoma	2	+	–	+/-	–	0					0					
Intraductal carcinoma	1	+	–	+	–	0					0					
Undifferentiated carcinoma	1	+	–	+/-	–	0					0					
Total	12	12/12	0/12	9/12	0/12	0					0					
Pancreas																
Adenocarcinoma	8	++	–	+	–	–	++	+	+	+	–	+	+/-	+	–	
Neuroendocrine tumors	4	+	–	–	–	–	+++	–	+++	–	–	++	–	+++	–	
Metastases of melanoma	1	+	–	–	–	0					0					
Total	13	13/13	0/13	8/13	0/13	2	2/2	½	2/2	1/2	2	2/2	0/2	2/2	0/2	
Lung																
Adenocarcinoma	7	+	–	+	+/-	0					0					
Squamocellular carcinoma	8	++	+/-	+	–	0					0					
Large-cell carcinoma	2	+	++	++	–	0					0					
Mesothelioma	1	+	–	+	–	–	++	+++	++	+	–	+/-	+++	++	+/-	
Metastases of colon adenocarcinoma	1	+	–	+/-	+	0					0					
Total	19	19/19	1/19	17/19	0/19	1	1/1	1/1	1/1	1/1	1	0/1	1/1	1/1	0/1	
Stomach																
Gastric adenocarcinoma	3	+	+	–	–	3	++	++	+/-	–	3	++	++	+/-	–	
Total	3	3/3	3/3	0/3	0/3	3	3/3	3/3	0/3	0/3	3	3/3	3/3	0/3	0/3	
Kidney																
Clear cell carcinoma	14	+++	++	–	–	0					0					
Papillary cell carcinoma	2	+	+/-	–	–	0					0					
Adenocarcinoma	1	–	++	+/-	–	0					0					
Oncocytoma	1	+	–	–	–	0					0					
Urothelial carcinoma of pelvis	1	+++	–	+/-	+	0					0					
Total	19	7/7	0/7	2/7	1/19	0					0					
Corticoadreno gland																
Surrenal carcinoma	1	+	–	–	–	0					0					
Total	1	1/1	0/1	0/1	0/1	0					0					
Soft tissues																
Solitary fibrous tumor	1	+	–	–	–	2	++	–	–	–	2	+	–	–	–	
Sarcoma	1	++	–	+	–	2	++	–	+	–	2	++	–	+	–	
Liposarcoma	2	++	–	+/-	–	3	+	+/-	+	–	3	+	+/-	+/-	–	
Osteosarcoma	1	++	–	++	+/-	1	++	+/-	++	+	1	++	–	++	+	
Angiomyolipoma	1	+	–	–	–	–	+	–	–	–	–	+	–	–	–	
pNET	1	+++	–	+/-	+	–	+++	–	+/-	–	–	++	–	–	–	
Total	7	7/7	0/7	0/19	1/19	10	10/10	0/10	6/10	1/10	10	10/10	0/10	3/10	1/10	
Thyroid																
Papillary carcinoma	1	++	+	+	–	1	+	+	++	–	1	+	+	+	–	
Total	1	1/1	1/1	1/1	0/1	1	1/1	1/1	1/1	0/1	1	1/1	1/1	1/1	0/1	
Nervous system																
Glioblastoma	1	++	–	+/-	–	2	+++	–	+/-	–	2	+++	–	+/-	–	
Paraganglioma	1	++	–	++	–	2	++	+/-	+	–	2	+	–	+	–	
Total	2	2/2	0/2	1/2	0/2	4	4/4	0/4	2/4	0/4	4	4/4	0/4	2/4	0/4	
Total	101	99/101	24/101	59/101	9/101	24	24/24	6/24	15/24	3/24	24	23/24	5/24	12/24	1/24	
%		(98.0)	(23.8)	(58.4)	(8.9)		(100)	(25.0)	(62.5)	(12.5)		(95.8)	(20.8)	(50.0)	(4.2)	

Table 2. Immunohistochemical Analysis of CD13 Expression in 32 Inflammatory Tissue Specimens

| | Monoclonal Antibody | | | | | | | | |
| | WM15 | | | BF10 | | | 3D8 | | |
Tissues	Vessels	Stroma	Tissue	Vessels	Stroma	Tissue	Vessels	Stroma	Tissue
Skin	5/7	5/7	0/7	4/11	8/11	0/11	4/11	8/11	0/11
Tonsil	1/1	1/1	0/1	1/1	1/1	0/1	1/1	1/1	0/1
Total	6/8	6/8	0/8	5/12	9/12	0/12	5/12	9/12	0/12
%	(75.0)	(75.0)	(0.0)	(41.7)	(75.0)	(0.0)	(41.7)	(75.0)	(0.0)

Table 3. Immunohistochemical Analysis of CD13 Expression in 58 Tissue-Normal Tissue Specimens

| | Monoclonal Antibody | | | | | | | | |
| | WM15 | | | BF10 | | | 3D8 | | |
Tissues	Vessels	Stroma	Tissue	Vessels	Stroma	Tissue	Vessels	Stroma	Tissue
Skin	0/1	0/1	0/1	0/1	0/1	0/1	0/1	0/1	0/1
Liver	3/7	6/7	7/7	3/5	5/5	5/5	3/5	5/5	5/5
Bowel	0/9	5/9	0/9	0/3	3/3	3/3	0/3	3/3	3/3
Breast	0/2	0/2	0/2						
Pancreas	0/2	0/2	0/2	1/1	1/1	1/1	1/1	1/1	0/1
Lung	0/4	1/4	0/4						
Kidney	0/4	0/4	4/4						
Stomach	0/2	0/2	0/2	0/2	0/2	1/2	0/2	0/2	0/2
Thyroid	0/1	0/1	0/1	0/1	0/1	0/1	0/1	0/1	0/1
Total	3/32	12/32	11/32	4/13	9/13	10/13	4/13	9/13	8/13
%	(9.3)	(37.5)	(34.4)	(30.7)	(69.2)	(76.9)	(30.7)	(69.2)	(61.5)

washed twice in PBS with 2% FBS and incubated with anti-CD31, anti-CD45, and the three anti-CD13 mAbs (WM15, BF10, and 3D8) for 30 min at 4C. After washing twice, cells stained with the anti-CD13 mAbs were incubated with a goat F(ab′)2 anti-mouse PE-conjugated IgG (Southern Biotech, Birmingham, AL) for 30 min at 4C; after washing twice, cells were finally suspended in PBS with 2% FBS for analysis (FlowJo Software, version 7.2.2; Tree Star Inc., Ashland, OR). To obtain a reliable $CD31^+CD45^-$ population gating, at least 5×10^5 cells were acquired for analysis.

Activated exponentially growing HUVEC (2×10^5) were detached with trypsin/EDTA, centrifuged at 1200 rpm for 5 min, and then incubated with either mouse anti-human AlexaFluor 488-endoglin (CD105, IgG_1, clone SN6; Serotec, Kidlington, UK) or anti-CD13 mAbs, testing each of the three clones (WM15, BF10, and 3D8), as above described.

Results

Tumor Tissues

Immunohistochemical analysis with WM15, BF10, and 3D8 mAbs was performed on 149 cases of different tumors (Table 1). Results are detailed below considering the three main neoplastic tissue components: tumor vessels, tumor stroma, and neoplastic cells. In addition, the three mAbs were tested in endothelial cells of two colon adenocarcinoma fresh tissue samples using flow cytometry.

CD13 expression in tumor vessels. WM15, BF10, and 3D8 mAbs detected CD13 in almost all vessels in tumor tissues (WM15, 99/101, 98.0%; BF10, 24/24, 100%; 3D8, 23/24, 95.8%). WM15 revealed almost all capillaries in tumor tissues, whereas arteries and venules were only occasionally decorated. In particular, it bound small intratumor and peritumor vessels of bowel (12/13) and pancreas (13/13) adenocarcinomas, breast carcinomas (12/12), lung squamocellular carcinomas (8/8), renal cell carcinomas (18/19), papillary carcinoma of thyroid (1/1), soft tissue tumors (7/7), and glioblastoma (1/1) specimens (Figure 1). WM15 did not stain tumor vasculature in only two cases: one colon adenocarcinoma and one renal cell carcinoma.

The immunoreactivity of BF10 and 3D8 was quite different: They reacted with endothelia of large vessels and only partially with capillaries. In addition, the signal produced by BF10 was often more intense and often less specific for intratumor
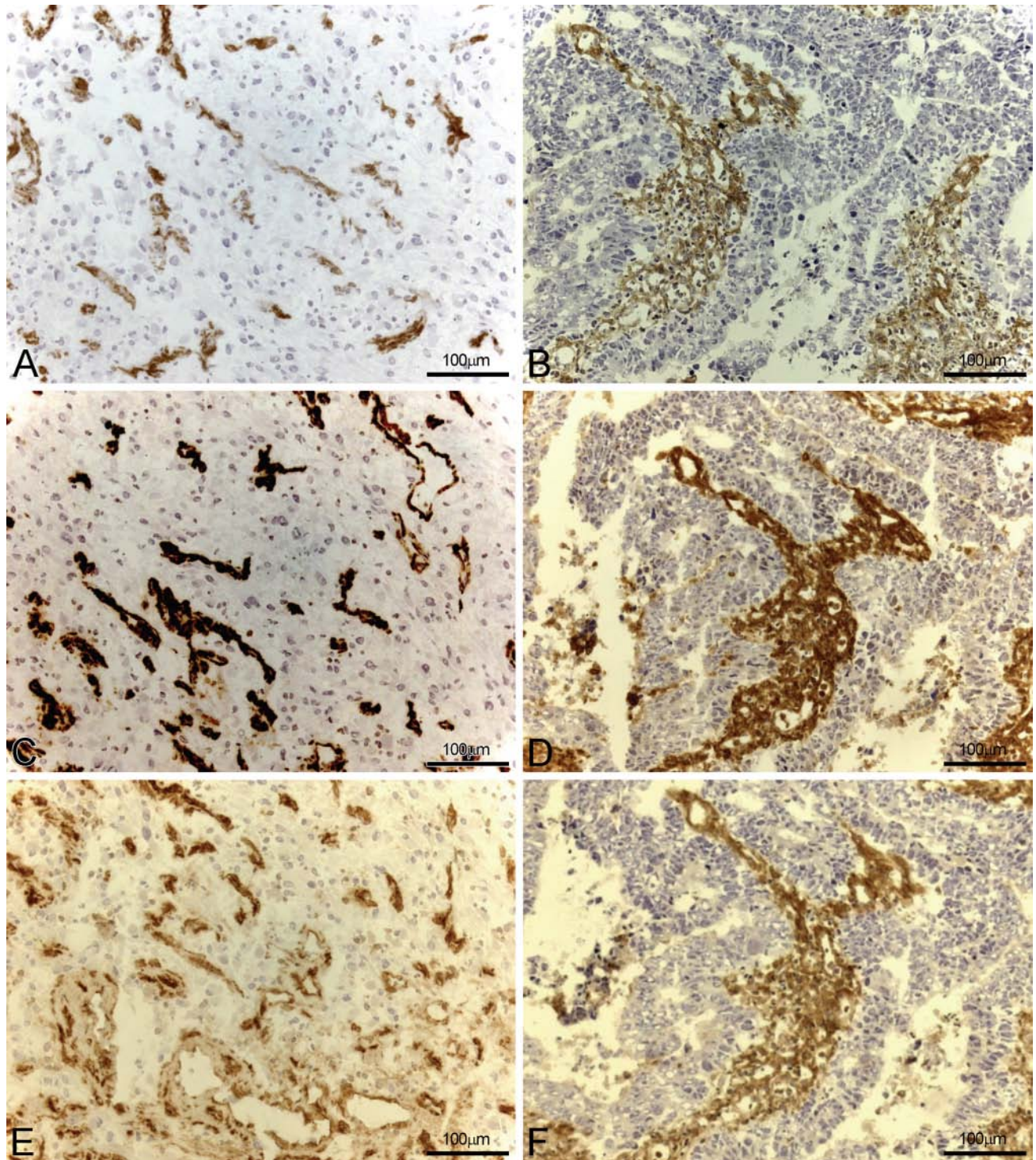
Figure 1. CD13 expression was investigated in glioblastoma (A, C, and E) and colon carcinoma (B, D, and F) specimens using three different monoclonal antibodies (mAbs): WM15 (A and B), BF10 (C and D), and 3D8 (E and F). In both tumor histotypes, the three mAbs stained stroma and tumor vessels, with WM15 preferentially highlighting small tumor vessels.

and peritumor vessels than that produced by WM15. In particular, BF10 detected almost all vessels in gastric (3/3), bowel (3/3), and pancreas (2/2) adenocarcinomas; mesothelioma (1/1); soft tissue tumors (10/10); and glioblastoma (1/1)

specimens (Figure 1). Although the staining patterns of BF10 and 3D8 were similar in most tissues, the intensity of 3D8 staining was weaker than that of BF10. In particular, 3D8 immunorevealed tumor large vessels in colon (3/3) and gastric
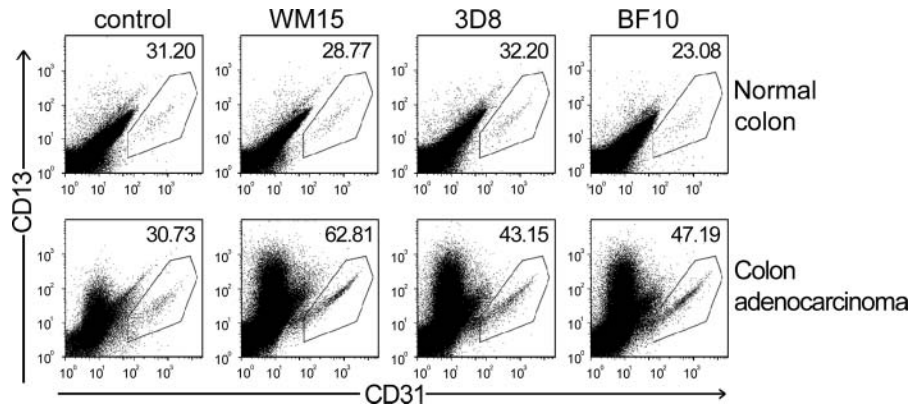
Figure 2. Flow cytometry analysis on CD31$^+$CD45$^-$ endothelial cells obtained from homogenized human tissue specimens of paired normal colon (upper dot-plot panels) and colon adenocarcinoma (lower dot-plot panels; *n* = 2) stained with isotopic control, WM15, 3D8, and BF10 monoclonal antibodies. CD31 expression is shown on the x-axis and the region in each dot-plot panel corresponds to gated CD31$^+$CD45$^-$ cells; CD13 expression is shown on the y-axis, and the number at the upper-right corner in each dot-plot panel corresponds to the CD13 median fluorescence intensity (MFI).

(3/3) adenocarcinomas, glioblastoma (2/2), and soft tissue tumors (10/10). Differently from BF10, 3D8 did not detect tumor vasculature in mesothelioma specimen.

Finally, the three mAbs stained CD31$^+$CD45$^-$ endothelial cells obtained homogenizing fresh colon adenocarcinoma tissue samples, and WM15 showed the highest median fluorescence intensity (MFI; Figure 2).

CD13 expression in tumor stroma. All three antibodies immunorevealed the tumor stroma in about half of neoplastic tissues (WM15, 59/101, 58.4%; BF10, 15/24, 62.5%; 3D8, 12/24, 50.0%). In particular, WM15 diffusely stained fibroblasts and connective tissue in hepatocarcinoma (9/11), colorectal (12/13), and pancreas (8/8) adenocarcinoma; lung adenocarcinoma (7/7); and squamocellular carcinoma (8/8) specimens (Figure 1). With a staining pattern similar to that of WM15, BF10 and 3D8 decorated connective tissues in colon and pancreas adenocarcinoma, mesothelioma, osteosarcoma, and thyroid papillary carcinoma specimens (Figure 1).

CD13 Expression in Neoplastic Cells. The three antibodies immunorevealed some tumor cell types (WM15 24/101, 23.8%; BF10 6/24, 25.0%; 3D8 5/24, 20.8%). In particular, WM15 stained tumor cells in kidney carcinoma (14/17), mesothelioma (1/1; Figure 3A, B), hepatocarcinoma (2/2; Figure 3C, D), gastric adenocarcinoma (3/3), and thyroid papillary carcinoma (1/1). Likewise, BF10 and 3D8 stained neoplastic cells in gastric adenocarcinoma, (3/3), mesothelioma (1/1), and in thyroid papillary carcinoma (1/1); BF10 also stained cancer cells of pancreas adenocarcinoma (1/1).

CD13 (WM15) and CD31 localization in tumor vessels. To establish the exact localization of CD13 in tumor endothelial cells, an immunofluorescence staining was performed with WM15 and CD31 antibodies. As shown in Figure 3E, both CD31 and WM15 stained tumor endothelial cells; however, with different patterns. CD31 bound to the luminal border of

tumor blood vessels, whereas WM15 preferentially stained the extraluminal border of endothelial cells and some auxiliary cells, like pericytes.

Inflammatory Lesions

The immunoreactivity of WM15, BF10, and 3D8 mAbs with vessels, stroma, and parenchyma was also investigated in 32 inflammatory lesions (Table 2).

CD13 expression in inflammation-associated vessels. The three antibodies stained vessels in about half of inflammatory lesions (WM15 6/8, 75.0%; BF10 5/12, 41.7%; 3D8 5/12, 41.7%). In particular, WM15 decorated capillaries and only partially large vessels in 5/7 inflammatory skin and 1/1 tonsil sections. BF10 and 3D8 produced almost identical results, staining vessels of dermo-epidermal junction in 4/11 inflamed skin and 1/1 tonsil sections (Figure 4).

CD13 expression in stroma. WM15 stained stroma of 5/7 inflamed skin and 1/1 tonsil sections, whereas BF10 and 3D8 immunorevealed fibroblasts and connective tissues in 8/11 inflammatory skin and 1/1 tonsil specimens.

CD13 expression in inflammatory cells and epithelia. WM15, BF10, and 3D8 neither stained epithelia nor lymphoid population in all inflammatory lesions tested. Of note, all antibodies weakly and occasionally immunorevealed inflammatory cells (macrophages, dendritic cells, whereas lymphocytes resulted always negative), as expected.

Normal Tissues

We investigated the immunoreactivity of WM15, BF10, and 3D8 mAbs also in 58 normal tissue samples (Table 3). In addition, the three mAbs were tested in endothelial cells of two normal colon fresh tissue samples and in HUVEC using flow cytometry.
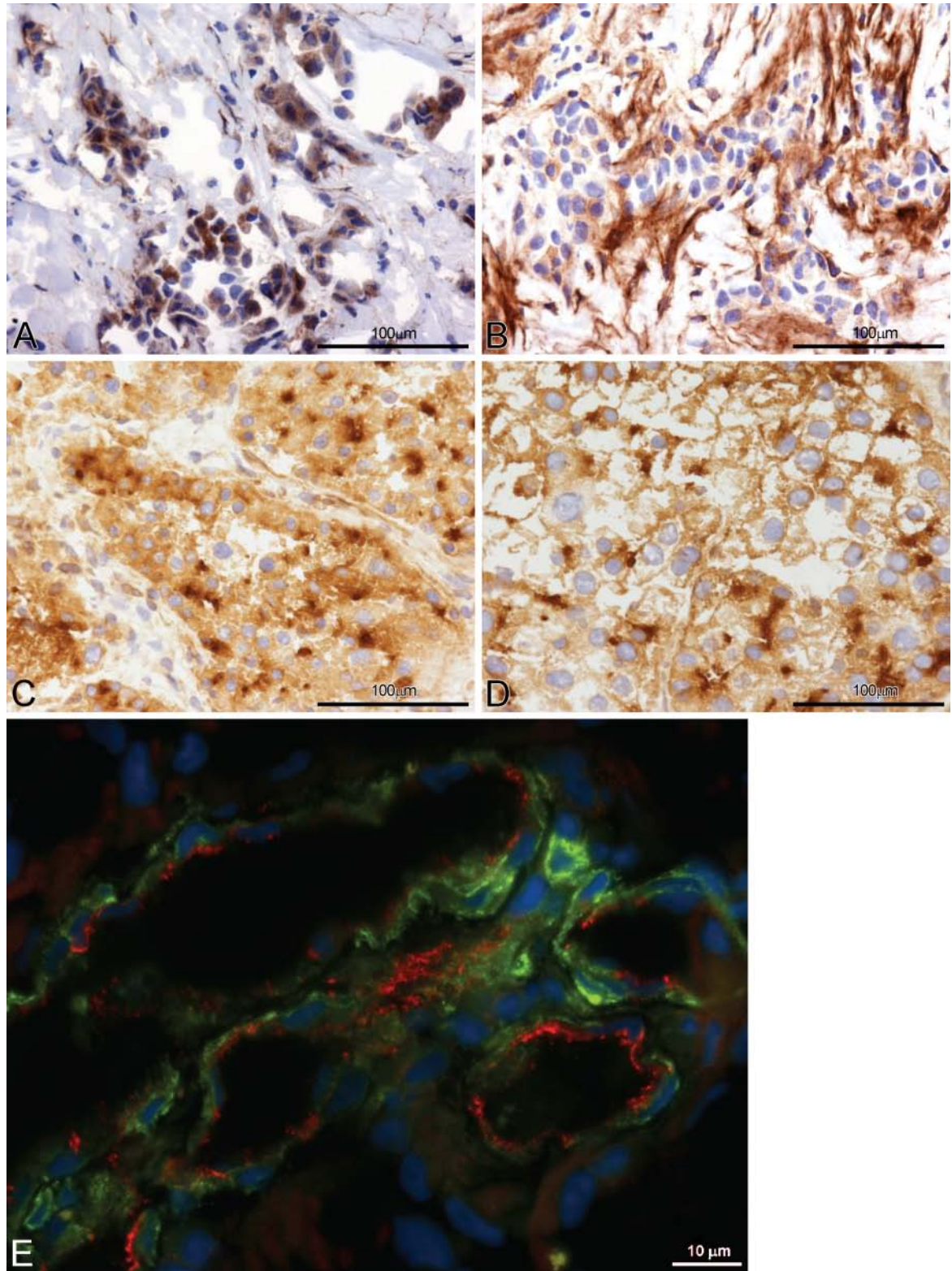
Figure 3. (A, B) CD13 expression in neoplastic cells (A), stroma, and vessels (B) with monoclonal antibody (mAb) WM15 in different areas of a case of mesothelioma. (C, D) CD13 expression in two cases of hepatocellular carcinoma with mAb WM15, showing membrane, cytoplasmic, and canalicular accentuation of staining as well as sinusoidal staining. (E) CD13 (WM15) and CD31 localization on endothelial cells of tumor blood vessels in glioblastoma, showing CD31 (red) on the vessel lumen and CD13 (green, WM15 mAb) on the abluminal side; nuclei are shown in blue (DAPI).
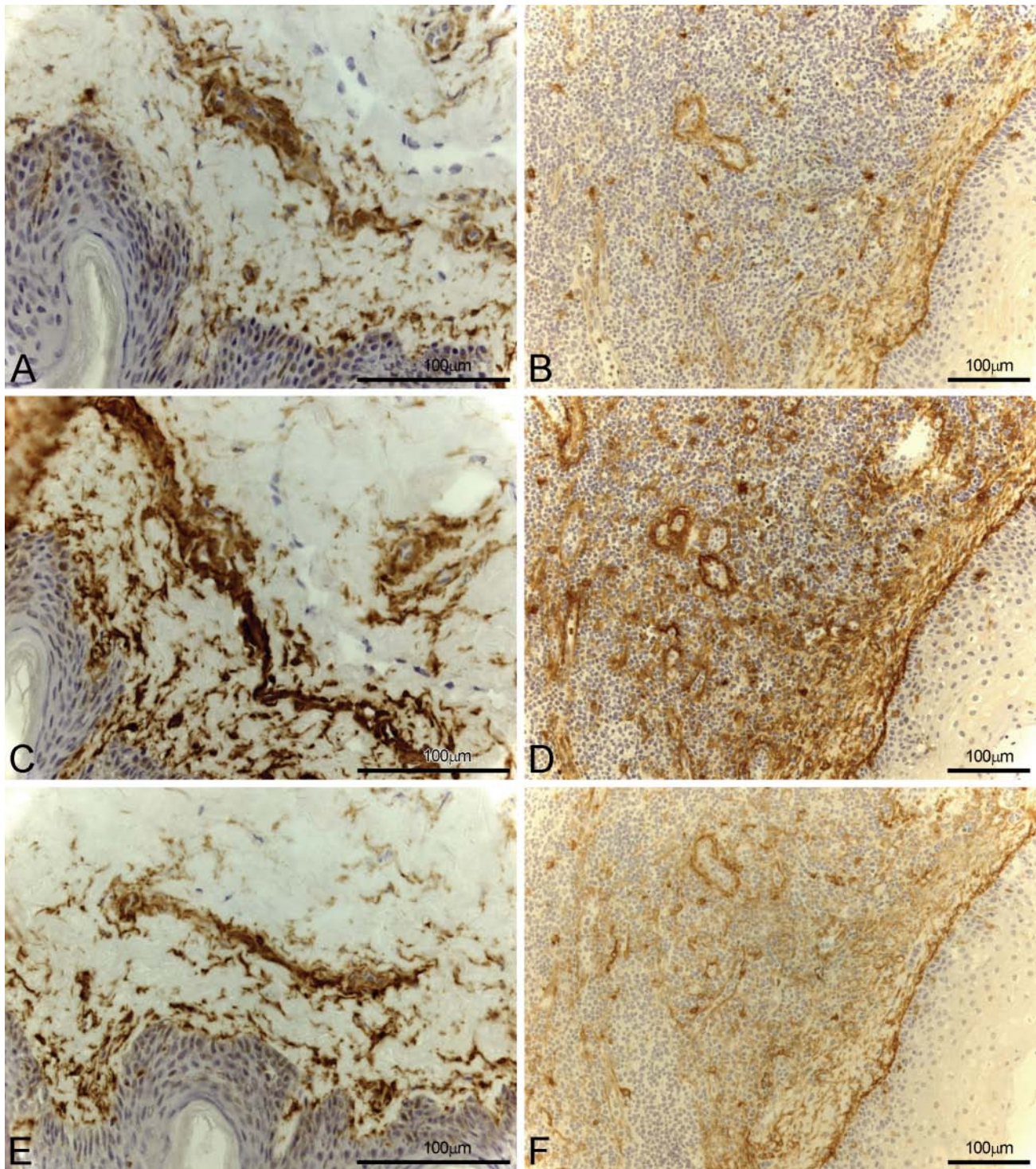
Figure 4. CD13 expression in inflammatory skin (A, C, and E) and tonsil (B, D, and F) with the three different monoclonal antibodies (mAbs): WM15 (A, B), BF10 (C, D), and 3D8 (E, F). All mAbs stained stroma and vessels along with some inflammatory cells.

CD13 expression in vessels. The antibodies stained blood vessels in a small percentage of normal tissues (WM15 3/32, 9.3%; BF10 4/13, 30.7%; 3D8 4/13, 30.7%; Figure 5). Of note, WM15 stained blood vessels in only 3/32 cases: in particular, WM15 stained sinusoids of 3/7 liver sections while neither stained centrolobular vein nor veins and arteries of portal space. Likewise, 3D8 and BF10 decorated only a small percentage of blood vessels (BF10 4/13, 3D8 4/13;
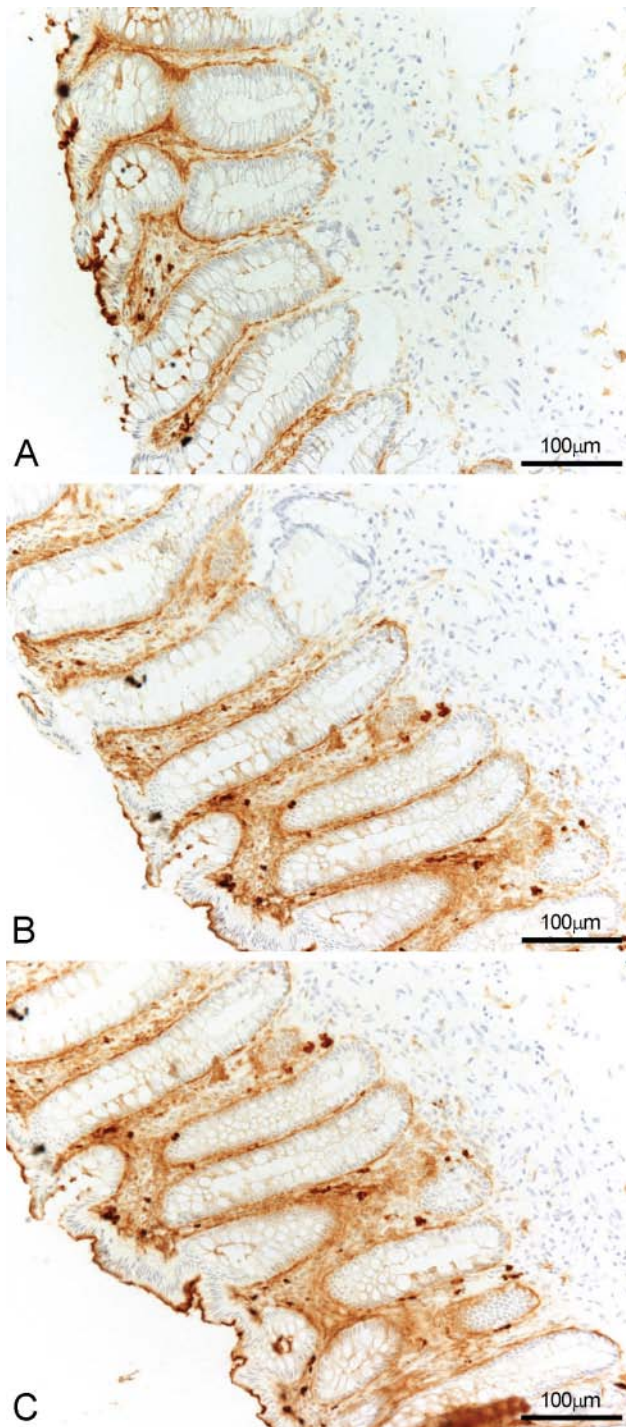
Figure 5. CD13 expression in normal colon with three different mAbs: WM15 (A), BF10 (B), and 3D8 (C). All monoclonal antibodies (mAbs) stained pericryptal fibroblasts, some inflammatory cells and the luminal borders of glandular epithelium. WM15 does not stain lamina propria vessels, whereas some reactivity is detected with both BF10 and 3D8 mAbs.

Figure 5). At flow cytometry, the three mAbs failed to stain CD31$^+$CD45$^-$ endothelial cells obtained homogenizing

fresh normal colon tissue samples (Figure 2), whereas they stained HUVEC with a similar intensity (data not shown). This is not surprising because HUVEC were exponentially growing and activated, as indicated by their expression of endoglin/CD105 (data not shown).

CD13 expression in stroma. WM15 bound the stroma in 12 of 32 specimens (37.5%): six liver, five bowel (basal membrane, fibroblasts, and in particular pericryptal fibroblasts), and one lung (connectival septs) specimen. BF10 and 3D8 stained stroma in liver, pancreas, and bowel specimens.

CD13 expression in epithelia. WM15 immunoreacted with normal epithelial cells in liver (hepatocytes and biliary ducts) and kidney (proximal tubules and Bowman capsule) specimens. Weak and variable staining was observed on the luminal border of gastrointestinal, mammary, and bronchial epithelia. Both BF10 and 3D8 stained liver and bowel epithelium, whereas only BF10 stained acinar structure and ducts of pancreas and the epithelium of stomach. Pancreatic endocrine cells were negative. All antibodies occasionally stained macrophages and dendritic cells present in the tissue specimens, as expected.

Discussion

Several studies investigated the expression of CD13 in various tissues using different mAbs obtaining varying results (Palmieri et al. 1985; Drexler 1987; Look et al. 1989; Ashmun and Look 1990; Ashmun et al. 1992; Kunz et al. 1994; Riemann et al. 1999). Among these, some reports showed that different anti-CD13 antibodies can recognize diverse forms of CD13 in normal epithelial cells, tumor-associated vessels, and myeloid cells (Curnis, et al. 2002; Pasqualini et al. 2000). The structural determinants responsible for differential binding of anti-CD13 antibodies to CD13 are still unclear. It has been suggested that differential O-glycosylation generates at least five forms of CD13 that are variably recognized by antibodies, likely because of diverse masking of protein epitopes (O'Connel et al. 1991). In addition, CD13 may undergo posttranslational modifications in tumor cells that may uncover an epitope, which can be recognized by specific mAbs, which is masked in normal tissues.

In the present study, we observed that although all antibodies tested, including WM15, 3D8, and BF10, stained vessels in most neoplastic tissues and tumor stroma in about half of the samples, the pattern of reactivity significantly varied among them, particularly between WM15 on one hand and BF10 and 3D8 on the other hand. As a matter of fact, WM15 immunodetected almost all intratumor and peritumor capillaries, whereas it only occasionally detected arteries and venules. This antibody also stained tumor cells of some histotypes, consistent with previous reports showing CD13 expression in non–small-cell lung cancer (Ito

et al. 2009) and in hepatocellular (Rocken et al. 2005), ovarian (Surowiak et al. 2006; Terauchi et al. 2007), gastric (Kawamura et al. 2007), and pancreatic carcinomas (Ikeda et al. 2003). At variance, the immunoreactivity of BF10 and 3D8 significantly differed from that of WM15. First, the signal produced by BF10 was always more intense but less restricted to tumor vessels than that produced by WM15. Although the staining patterns of BF10 and 3D8 were similar in most tissues, the intensity of BF10 staining was greater than that of 3D8. Second, both BF10 and 3D8 bound to the endothelium of almost all arteries and venules and only partially to that of tumor capillaries. In agreement with these data, the three mAbs stained CD31$^+$CD45$^-$ endothelial cells of colon adenocarcinoma tissue specimens. Considering that conceivably, these tumor samples contained more capillaries than arteries and venules, it is interesting to note that the CD13 MFI was higher with WM15 than using BF10 and 3D8, consistent with the different preferential staining of WM15 for tumor capillaries.

Different results were obtained with inflammatory lesions, as in this case the three antibodies stained vessels in only half of the tissues tested. Nevertheless, WM15, BF10, and 3D8 stained the stroma, and again, WM15 was more selective for capillaries, whereas BF10 and 3D8 reacted with large vessels and only partially with capillaries.

Of note, in normal tissues, the three antibodies stained only a small percentage of blood vessels (WM15: 9.3%; BF10: 30.7%; 3D8: 30.7%). A higher percentage value of reactivity (~50%) was present in liver vessels, conceivably due to the peculiar anatomic and functional characteristics of the sinusoidal endothelium and pericytes/hepatic stellate cells, which have unique regenerative potential and scavenger activity (Enomoto et al. 2004; Lee et al. 2007). Furthermore, these antibodies stained monocytes/macrophages, biliary ducts, kidney proximal tubules, and luminal surface of intestinal epithelia although to a different extent (WM15 34.4%; BF10 76.9%; 3D8 61.5%). Of note, only BF10 stained acinar and ductal cells of pancreas. These results on normal tissues are in line with those of previous reports (Ashmun and Look 1990; Taylor 1993; Dixon et al. 1994; Piela-Smith and Korn 1995; Riemann et al. 1997; Riemann et al. 1999; Bauvois and Dauzonne 2006). Overall, our results provide support for the concept that different immunoreactive forms of CD13 are present in different tissues in normal and pathological conditions. Remarkably, they also indicate that CD13 is expressed by vessels in neoplastic and some inflammatory lesions, with minimal reactivity in the vasculature of normal tissues.

Previous studies investigated the role of CD13 in tumors. Some papers suggested that CD13 could be exploited as a diagnostic and prognostic marker in certain tumors, such as lung squamous cell carcinoma and other non–small-cell lung cancer, gastric and colon carcinoma, hepatocellular and pancreatic carcinoma, ovarian and cervical cancer (Hashida et al. 2002; Ikeda et al. 2003; Rocken et al. 2005;

Ichimura et al. 2006; Surowiak et al. 2006; Tokuhara et al. 2006; Kawamura et al. 2007; Terauchi et al. 2007; Yamashita et al. 2007; Tsukamoto 2008; Ito et al. 2009). More recently, other papers showed that CD13 plays multiple roles in angiogenesis (Pasqualini et al. 2000; Bhagwat et al. 2001; Bhagwat et al. 2003; Bauvois 2004; Bauvois and Dauzonne 2006; Fukasawa et al. 2006; Mahoney et al. 2007; Rangel et al. 2007; Yang et al. 2007; Mina Osorio 2008). Consistently, we observed that angiogenic/activated (CD105$^+$) exponentially growing HUVEC overexpressed CD13 and stained positive to the three anti-CD13 mAbs (data not shown), which in contrast did not stain CD31$^+$CD45$^-$ endothelial cells obtained homogenizing fresh normal colon tissue samples. In addition, it has been reported that CD13 is critical for the development of new blood vessels from existing vessels in pathological conditions (Rangel et al. 2007). Consistently, we demonstrated that CD13 is diffusely expressed in tumor vasculature and stroma and, in particular, that tumor capillaries—conceivably angiogenic ones— are efficiently recognized by WM15 and to a much lesser extent by BF10 and 3D8. Overall, these findings indicate that CD13 is up-regulated during angiogenesis, including the one occurring during inflammation and tumor growth, and that WM15 is selective for a CD13 form expressed by mostly angiogenic tumor neovasculature (i.e., tumor capillaries).

The enhanced expression of CD13 in vessels of pathologic tissues could have important implications for therapies based on CD13-positive vessel targeting (Arap et al. 1998a; Corti 2004; Corti and Ponzoni 2004), in particular for those based on the use of the NGR peptide as a CD13-targeting ligand (Curnis, Arrigoni, et al. 2002; Pasqualini et al. 2000). This peptide has been used for delivering various antitumor compounds, such as chemotherapeutic drugs, apoptotic peptides, viral particles, cytokines (Gregorc et al. 2009; Gregorc, Citterio, et al. 2010; Gregorc, Zucali, et al. 2010; Santoro, Pressiani, et al. 2010; Santoro, Rimassa, et al. 2010; van Laarhoven et al. 2010), and liposomes, to tumor vessels (Arap et al. 1998a, 1998b; Ellerby et al. 1999; Curnis et al. 2000; Liu et al. 2000; Grifman et al. 2001; Curnis, Sacchi, et al. 2002; Pastorino et al. 2003; Curnis et al. 2005; Garde et al. 2007). Among these, NGR-hTNF (www.molmed.com), which couples CNGRCG with hTNFα, is currently tested in phase 2 and 3 clinical trials (Gregorc et al. 2009; Gregorc, Citterio, et al. 2010; Gregorc, Zucali, et al. 2010; Santoro, Pressiani, et al. 2010; Santoro, Rimassa, et al. 2010; van Laarhoven et al. 2010). Our finding that CD13 is expressed in the vasculature of most of the tumors tested, but not of normal tissues, suggests that NGR-peptide conjugates could potentially target the vasculature of most solid tumors.

Although CD13 is expressed also by many normal cell types and tissues, such as biliary ducts, kidney proximal tubules, luminal surface of intestinal epithelia (Atherton

et al. 1992; Taylor 1993; Dixon et al. 1994; Chen et al. 1996; Bogenrieder et al. 1997; Riemann et al. 1999), previous papers demonstrated that the NGR peptide (Curnis, et al. 2002) can selectively bind a form expressed by the tumor vasculature (Curnis, et al. 2002; Pasqualini et al. 2000). Remarkably, the finding that CD13 is expressed also both in the vasculature of some inflammatory skins and tonsils and in angiogenic/activated HUVEC indicates that the vascular expression of CD13 may not be limited to tumors. Whether this form of CD13 is recognized by NGR peptides remains to be investigated.

In conclusion, although all antibodies tested in this study bind tumor vessels, WM15 binds almost all tumor capillaries and little or no large vessels, whereas BF10 and 3D8 bind large peritumor vessels and much less small vessels. Therefore, WM15 may be a good tool for detecting the CD13 form associated with the angiogenic tumor vasculature. This finding may be relevant for CD13-mediated vascular targeting therapies.

Acknowledgments

Literature Cited

Arap W, Kolonin MG, Trepel M, Lahdenranta J, Cardo-Vila M, Giordano RJ, Mintz PJ, Ardelt PU, Yao VJ, Vidal CI, et al. 2002. Steps toward mapping the human vasculature by phage display. Nat Med. 8:121-127.

Arap W, Pasqualini R, Ruoslahti E. 1998a. Cancer treatment by targeted drug delivery to tumor vasculature in a mouse model. Science. 279:377-380.

Arap W, Pasqualini R, Ruoslahti E. 1998b. Chemotherapy targeted to tumor vasculature. Curr Opin Oncol. 10:560-565.

Ashmun RA, Look AT. 1990. Metalloprotease activity of CD13/aminopeptidase N on the surface of human myeloid cells. Blood. 75:462-469.

Ashmun R, Shapiro LH, Look AT. 1992. Deletion of the zinc-binding motif of CD13/aminopeptidase N molecules results in loss of epitopes that mediate binding of inhibitory antibodies. Blood. 79:3344-3349.

Atherton AJ, Monaghan P, Warburton MJ, Gusterson BA. 1992. Immunocytochemical localization of the ectoenzyme aminopeptidase N in the human breast. J Histochem Cytochem. 40:705-710.

Bauvois B. 2004. Transmembrane proteases in cell growth and invasion: new contributors to angiogenesis? Oncongene. 23:317-329.

Bauvois B, Dauzonne D. 2006. Aminopeptidase-N/CD13 (EC 3.4.11.2) inhibitors: chemistry, biological evaluations, and therapeutic prospects. Med Res Rev. 26:88-130.

Bhagwat SV, Lahdenranta J, Giordano R, Arap W, Pasqualini R, Shapiro LH. 2001. CD13/APN is activated by angiogenic signals and is essential for capillary tube formation. Blood. 97:652-659.

Bhagwat SV, Petrovic N, Okamoto Y, Shapiro LH. 2003. The angiogenic regulator CD13/APN is a transcriptional target of Ras signaling pathways in endothelial morphogenesis. Blood. 101:1818-1826.

Bogenrieder T, Finstad CL, Freeman RH, Papandreou CN, Scher HI, Albino AP, Reuter VE, Nanus DM. 1997. Expression and localization of aminopeptidase A, aminopeptidase N, and dipeptidyl peptidase IV in benign and malignant human prostate tissue. Prostate. 33:225-232.

Chen H, Kinzer CA, Paul WE. 1996. p161, a murine membrane protein expressed on mast cells and some macrophages, is mouse CD13/aminopeptidase N. J Immunol. 157:2593-2600.

Corti A. 2004. Strategies for improving the anti-neoplastic activity of TNF by tumor targeting. Methods Mol Med. 98:247-264.

Corti A, Ponzoni M. 2004. Tumor vascular targeting with tumor necrosis factor alpha and chemotherapeutic drugs. Ann N Y Acad Sci. 1028:104-112.

Curnis F, Arrigoni G, Sacchi A, Fischetti L, Arap W, Pasqualini R, Corti A. 2002. Differential binding of drugs containing the NGR motif to CD13 isoforms in tumor vessels, epithelia, and myeloid cells. Cancer Res. 62:867-874.

Curnis F, Gasparri A, Sacchi A, Cattaneo A, Magni F, Corti A. 2005. Targeted delivery of IFNgamma to tumor vessels uncouples antitumor from counterregulatory mechanisms. Cancer Res. 65:2906-2913.

Curnis F, Sacchi A, Borgna L, Magni F, Gasparri A, Corti A. 2000. Enhancement of tumor necrosis factor alpha antitumor immunotherapeutic properties by targeted delivery to aminopeptidase N (CD13). Nat Biotechnol. 18:1185-1190.

Curnis F, Sacchi A, Corti A. 2002. Improving chemotherapeutic drug penetration in tumors by vascular targeting and barrier alteration. J Clin Invest. 110:475-482.

Dixon J, Kaklamanis L, Turley H, Hickson ID, Leek RD, Harris AL, Gatter KC. 1994. Expression of aminopeptidase-n (CD 13) in normal tissues and malignant neoplasms of epithelial and lymphoid origin. J Clin Pathol. 47:43-47.

Drexler HG. 1987. Classification of acute myeloid leukemias—a comparison of FAB and immunophenotyping. Leukemia. 1:697-705.

Ellerby HM, Arap W, Ellerby LM, Kain R, Andrusiak R, Rio GD, Krajewski S, Lombardo CR, Rao R, Ruoslahti E, et al. 1999. Anti-cancer activity of targeted pro-apoptotic peptides. Nat Med. 5:1032-1038.

Enomoto K, Nishikawa Y, Omori Y, Tokairin T, Yoshida M, Ohi N, Nishimura T, Yamamoto Y, Li Q. 2004. Cell biology and pathology of liver sinusoidal endothelial cells. Med Electron Microsc. 37:208-215.

Fukasawa K, Fujii H, Saitoh Y, Koizumi K, Aozuka Y, Sekine K, Yamada M, Saiki I, Nishikawa K. 2006. Aminopeptidase N (APN/CD13) is selectively expressed in vascular endothelial cells and plays multiple roles in angiogenesis. Cancer Lett. 243:135-143.

Garde SV, Forté AJ, Ge M, Lepekhin EA, Panchal CJ, Rabbani SA, Wu JJ. 2007. Binding and internalization of NGR-peptide-targeted liposomal doxorubicin (TVT-DOX) in CD13-expressing cells and its antitumor effects. Anticancer Drugs. 18:1189-1200.

Gregorc V, Citterio G, Vitali G, Spreafico A, Scifo P, Borri A, Donadoni G, Rossoni G, Corti A, Caligaris-Cappio F, et al. 2010. Defining the optimal biological dose of NGR-hTNF, a selective vascular targeting agent, in advanced solid tumours. Eur J Cancer. 46:198-206.

Gregorc V, Santoro A, Bennicelli E, Punt CJ, Citterio G, Timmer-Bonte JN, Caligaris Cappio F, Lambiase A, Bordignon C, van Herpen CM. 2009. Phase Ib study of NGR-hTNF, a selective vascular targeting agent, administered at low doses in combination with doxorubicin to patients with advanced solid tumours. Br J Cancer. 101:219-224.

Gregorc V, Zucali PA, Santoro A, Ceresoli GL, Citterio G, De Pas TM, Zilembo N, De Vincenzo F, Simonelli M, Rossoni G, et al. 2010. Phase II study of asparagine-glycine-arginine-human tumor necrosis factor {alpha}, a selective vascular targeting agent, in previously treated patients with malignant pleural mesothelioma. J Clin Oncol. 28:2604-2611.

Grifman M, Trepel M, Speece P, Gilbert LB, Arap W, Pasqualini R, Weitzman MD. 2001. Incorporation of tumor-targeting peptides into recombinant adeno-associated virus capsids. Mol Ther. 3:964-975.

Hashida H, Takabayashi A, Kanai M, Adachi M, Kondo K, Kohno N, Yamaoka Y, Miyake M. 2002. Aminopeptidase N is involved in cell motility and angiogenesis: its clinical significance in human colon cancer. Gastroenterology. 122:376-386.

Ichimura E, Yamada M, Nishikawa K, Abe F, Nakajima T. 2006. Immunohistochemical expression of aminopeptidase N (CD13) in human lung squamous cell carcinomas, with special reference to Bestatin adjuvant therapy. Pathol Int. 56:296-300.

Ikeda N, Nakajima Y, Tokuhara T, Hattori N, Sho M, Kanehiro H, Miyake M. 2003. Clinical significance of aminopeptidase N/CD13 expression in human pancreatic carcinoma. Clin Cancer Res. 9:1503-1508.

Ito S, Miyahara R, Takahashi R, Nagai S, Takenaka K, Wada H, Tanaka F. 2009. Stromal aminopeptidase N expression: correlation with angiogenesis in non-small-cell lung cancer. Gen Thorac Cardiovasc Surg. 57:591-598.

Kawamura J, Shimada Y, Kitaichi H, Komoto I, Hashimoto Y, Kaganoi J, Miyake M, Yamasaki S, Kondo K, Imamura M. 2007. Clinicopathological significance of aminopeptidase N/CD13 expression in human gastric carcinoma. Hepatogastroenterology. 54:36-40.

Kunz J, Krause D, Kremer M, Dermietzel R. 1994. The 140-kDa protein of blood-brain barrier-associated pericytes is identical to aminopeptidase N. J Neurochem. 62:2375-2386.

Lee JS, Semela D, Iredale J, Shah VH. 2007. Sinusoidal remodeling and angiogenesis: a new function for the liver-specific pericyte? Hepatology. 45:817-825.

Liu L, Anderson WF, Beart RW, Gordon EM, Hall FL. 2000. Incorporation of tumor vasculature targeting motifs into moloney murine leukemia virus env escort proteins enhances retrovirus binding and transduction of human endothelial cells. J Virol. 74:5320-5328.

Look AT, Ashmun RA, Shapiro LH, Peiper SC. 1989. Human myeloid plasma membrane glycoprotein CD13 (gp150) is identical to aminopeptidase N. J Clin Invest. 83:1299-1307.

Luan Y, Wu W. 2007. The structure and main functions of aminopeptidase N. Curr Med Chem. 14:639-647.

Mahoney KM, Petrovic N, Schacke W, Shapiro LH. 2007. CD13/APN transcription is regulated by the proto-oncogene c-Maf via an atypical response element. Gene. 403:178-187.

Mina-Osorio P. 2008. The moonlighting enzyme CD13: old and new functions to target. Trends Mol Med. 14:361-371.

O'Connel P, Gerkis V, D'Apice AJ. 1991. Variable *O*-glycosylation of CD13 (aminopeptidase N). J Biol Chem. 266:4593-4597.

Palmieri FE, Petrelli JJ, Ward PE. 1985. Vascular, plasma membrane aminopeptidase M: metabolism of vasoactive peptides. Biochem Pharmacol. 34:2309-2317.

Pasqualini R, Koivunen E, Kain R, Lahdenranta J, Sakamoto M, Stryhn A, Ashmun RA, Shapiro LH, Arap W, Ruoslahti E. 2000. Aminopeptidase N is a receptor for tumor-homing peptides and a target for inhibiting angiogenesis. Cancer Res. 60:722-727.

Pasqualini R, Ruoslahti E. 1996. Organ targeting in vivo using phage display peptide libraries. Nature. 380:364-366.

Pastorino F, Brignole C, Marimpietri D, Cilli M, Gambini C, Ribatti D, Longhi R, Allen TM, Corti A, Ponzoni M. 2003. Vascular damage and anti-angiogenic effects of tumor vessel-targeted liposomal chemotherapy. Cancer Res. 63:7400-7409.

Piela-Smith TH, Korn JH. 1995. Aminopeptidase N: a constitutive cell-surface protein on human dermal fibroblasts. Cell Immunol. 162:42-48.

Rangel R, Sun Y, Guzman-Rojas L, Ozawa MG, Sun J, Giordano RJ, Van Pelt CS, Tinkey PT, Behringer RR, Sidman RL, et al. 2007. Impaired angiogenesis in aminopeptidase N-null mice. Proc Natl Acad Sci U S A. 104:4588-4593.

Razak K, Newland AC. 1992a. Induction of CD13 expression on fresh myeloid leukaemia: correlation of CD13 expression with aminopeptidase-N activity. Leuk Res. 16:625-630.

Razak K, Newland AC. 1992b. The significance of aminopeptidases and haematopoietic cell differentiation. Blood Rev. 6:243-250.

Riemann D, Kehlen A, Langner J. 1999. CD13—not just a marker in leukemia typing. Immunol Today. 20:83-88.

Riemann D, Kehlen A, Thiele K, Lohn M, Langner J. 1997. Induction of aminopeptidase N/CD13 on human lymphocytes after adhesion to fibroblast-like synoviocytes, endothelial cells, epithelial cells, and monocytes/macrophages. J Immunol. 158:3425-3432.

Rocken C, Licht J, Roessner A, Carl-McGrath S. 2005. Canalicular immunostaining of aminopeptidase N (CD13) as a diagnostic marker for hepatocellular carcinoma. J Clin Pathol. 58: 1069-1075.

Santoro A, Pressiani T, Citterio G, Rossoni G, Donadoni G, Pozzi F, Rimassa L, Personeni N, Bozzarelli S, Rossoni G, et al. 2010. Activity and safety of NGR-hTNF, a selective vascular-targeting agent, in previously treated patients with advanced hepatocellular carcinoma. Br J Cancer. 103:837-844.

Santoro A, Rimassa L, Sobrero AF, Citterio G, Sclafani F, Carnaghi C, Pessino A, Caprioni F, Andretta V, Tronconi M, et al. 2010. Phase II study of NGR-hTNF, a selective vascular targeting agent, in patients with metastatic colorectal cancer after failure of standard therapy. Eur J Cancer. 46:2746-2752.

Surowiak P, Drag M, Materna V, Suchocki S, Grzywa R, Spaczynski M, Dietel M, Oleksyszyn J, Zabel M, Lage H. 2006. Expression of aminopeptidase N/CD13 in human ovarian cancers. Int J Gynecol Cancer. 16:1783-1788.

Taylor A. 1993. Aminopeptidases: structure and function. FASEB J. 7:290-298.

Terauchi M, Kajiyama H, Shibata K, Ino K, Nawa A, Mizutani S, Kikkawa F. 2007. Inhibition of APN/CD13 leads to suppressed progressive potentila in ovarian carcinoma cells. BMC Cancer. 7:140.

Tokuhara T, Hattori N, Ishida H, Hirai T, Higashiyama M, Kodama K, Miyake M. 2006. Clinical significance of aminopeptidase N in non-small cell lung cancer. Clin Cancer Res. 12:3971-3978.

Tsukamoto H, Shibata K, Kajiyama H, Terauchi M, Nawa A, Kikkawa F. 2008. Aminopeptidase N (APN)/CD13 inhibitor, Ubenimex, enhances radiation sensitivity in human cervical cancer. BMC Cancer. 8:74.

van Laarhoven HW, Fiedler W, Desar IM, van Asten JJ, Marreaud S, Lacombe D, Govaerts AS, Bogaerts J, Lasch P, Timmer-Bonte JN, et al. 2010. Phase I clinical and magnetic resonance imaging study of the vascular agent NGR-hTNF in patients with advanced cancers (European Organization for Research and Treatment of Cancer Study 16041). Clin Cancer Res. 16:1315-1323.

Wulfaenger J, Niedling S, Riemann D, Seliger B. 2008. Aminopeptidase N (APN)/CD13-dependent CXCR4 downregulation is associated with diminished cell migration, proliferation and invasion. Mol Membr Biol. 25:72-82.

Yamashita M, Kajiyama H, Terauchi M, Shibata K, Ino K, Nawa A, Mizutani S, Kikkawa F. 2007. Involvement of aminopeptidase N in enhanced chemosensitivity to paclitaxel in ovarian carcinoma in vitro and in vivo. Int J Cancer. 120:2243-2250.

Yang E, Shim JS, Woo HJ, Kim KW, Kwon HJ. 2007. Aminopeptidase N/CD13 induces angiogenesis through interaction with a pro-angiogenic protein, galectin-3. Biochem Biophys Res Commun. 363:336-341.